Turkish Journal of Earth Sciences

http://journals.tubitak.gov.tr/earth/

Research Article

Turkish J Earth Sci
(2019) 28: 470-477

doi:10.3906/yer-1808-6

Graphite in rocks of the Popigai impact crater: residual or retrograde?

Valentin AFANASIEV[1,*], Sergey GROMILOV[2,3], Valeri SONIN[1], Egor ZHIMULEV[1], Aleksei CHEPUROV[1]

[1]V.S. Sobolev Institute of Geology and Mineralogy, Siberian Branch of the Russian Academy of Sciences, Novosibirsk, Russia
[2]A.V. Nikolaev Institute of Inorganic Chemistry, Siberian Branch of the Russian Academy of Sciences, Novosibirsk, Russia
[3]Novosibirsk State University, Novosibirsk, Russia

Received: 03.08.2018 • **Accepted/Published Online:** 28.03.2019 • **Final Version:** 10.05.2019

Abstract: The concentration of diamond-bearing tagamite from the Popigai impact crater produces large amounts of graphite in addition to impact diamonds (1:100, respectively). The question arises of whether this is residual graphite not converted to diamond at the time of the Popigai impact or is a retrograde form resulting from back-conversion of impact diamond to graphite in a high-temperature tagamite melt. Experiments show that graphite from tagamite is a residual phase. Coexistence of lonsdaleite, cubic diamond, and single-crystal graphite within a limited volume may be due to different orientations of the graphite base plane relative to the impact stress direction. Thus, the diamond-bearing rocks may contain significant amounts of residual graphite, which is consistent with published evidence.

Key words: Impact crater, impact diamond, graphite, bulk graphitization, surface graphitization

1. Introduction

The Popigai impact crater is located in the northern Siberian craton at the boundary between the Krasnoyarsk region and Yakutia (Figure 1). The impact origin of the crater was proven in 1971 by Victor L. Masaitis (Masaitis, 1998), a prominent Russian geologist. His later discovery of abundant diamond inclusions in the crater rocks (impactites) attracted great interest to the Popigai crater.

Studies at the Popigai site in the course of 15 consecutive years provided constraints on the crater structure and the features of the discovered diamonds, and a special technology was developed for treatment of the diamond-bearing rocks and extraction of diamonds. The impact diamond turned out to possess 1.8–2.4 times greater abrasion strength than ordinary diamonds (Shul'zhenko et al., 2014). The exceptional properties of impact diamonds are due to their microstructure, which is an aggregate of nanometer cubic diamond and hexagonal lonsdaleite phases. However, studies of the Popigai crater and impact diamonds stopped in the mid-1980s, while the obtained results were classified as confidential. This status has recently been changed and the research may now continue to gain insights into many issues that remain unclear.

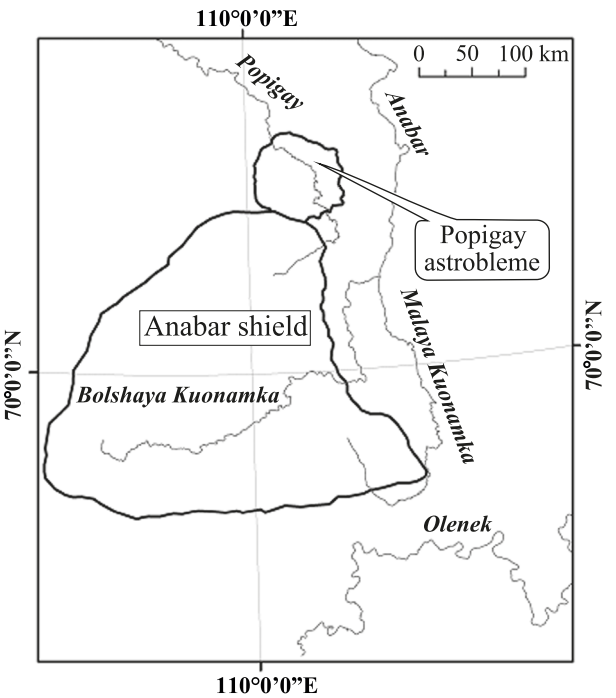

Figure 1. The scheme of the Popigai astrobleme location (Nalivkin, 2007). Scale is 1:2,500,000.

* Correspondence: avp-diamond@mail.ru

The predominant size of impact diamonds extracted from host rocks is in the range of 0.05–2.0 mm, with an average of 0.2 mm (Masaitis, 2014). In the placers occurring due to erosion of astrobleme rocks, diamonds of up to 12 mm were found. Diamonds are different shades of yellow, rarely uncolored or gray, black-gray, and black. The shape of impact diamonds is often similar to the original graphite: flattened plates, whose basal planes retain their twin-striation typical for graphite, and the side planes have a stepped structure. In addition, graphite is found in the form of leaf-like particles and their aggregates. It is assumed that graphite may be secondary and newly formed. The density of impact diamonds varies within the range of 3.2846–3.6127 g/cm^3. The isotope ratio δ13C ranges from –9.9‰ to –31.5‰. Research showed that impact diamonds match the isotopic composition of graphite from crystalline rocks of the Anabar massif (Galimov, 1984). Impact diamonds have yellow-orange luminescence under UV light (Yelisseyev et al., 2016).

One important issue concerns the origin of graphite in impactites, especially in tagamites (rocks remelted by the impact). Impact diamonds were derived from well-crystallized graphite found in gneisses of the Khapchan Group that crop out in the western and southwestern parts of the crater (Masaitis, 1998). The diamond contents vary strongly over the crater area and reach 100 carats per ton of bulk rock at one of the explored sites (the Skalnoe deposit). The reserves of this section of the Popigai crater are estimated at 140 billion carats, with an average grade of 23.23 carats per ton (Kryukov et al., 2016). However, any processing method (thermochemical decomposition, autoclaving, flotation, etc.) yields mostly graphite. Large amounts of diamond were extracted for engineering tests by flotation at a specially designed factory, while the ratio of diamond to graphite in the concentrate was about 1:100. The question arises of whether the graphite is residual, which escaped conversion to diamond during the impact event, or whether it is of retrograde origin produced by graphitization of impact diamond in a high-temperature silicate tagamite melt (Masaitis, 1998). This problem is also important because the diamonds contain inclusions of graphite (residual or retrograde?). The problem was studied by means of experimental graphitization of impact diamonds.

2. Materials and methods

Experiments were applied to graphite from a heavy mineral concentrate (HMC) sample (A), small grains of ~100 μm (sample B), and pieces of lamellar impact diamonds of about 1 mm (sample C).

The experiments were performed using a split-sphere multianvil apparatus with a high-pressure cell in the form of a rectangular prism of 20 × 20 × 23 mm made by compression of powdered ZrO_2, CaO, and MgO oxides, with a graphite cylindrical heater placed in a hole of 11 mm in diameter in the cell center. The heater had 0.5-mm-thick walls, and Mo rods and discs were used as electric contacts. The sample was insulated from the heater by a sleeve with 1-mm-thick walls on the sides and by 2-mm-thick pellets of MgO on the top and bottom.

Temperature was measured in each experiment with a $PtRh_6/PtRh_{30}$ thermocouple to an accuracy of ±25 °C. The temperature gradient in the cell was no greater than 15 °C/mm at 1500 °C. Pressure was measured with a manometer gauge to an accuracy of ±0.2 GPa according to the precalibrated correlation between the pressure in the cell and oil pressure in the hydraulic system of the apparatus. The pressure calibration was performed using the substances Bi and PbSe and by bracketing the quartz-coesite and graphite-diamond *P-T* equilibria (Kennedy and Kennedy, 1976; Hemingway et al., 1998). Correction for pressure increase in the cell during heating was applied for each experiment.

Samples of impact diamond were placed in a NaCl medium, which remains almost invariable during experiments and can be easily removed by dissolution in water afterwards to extract the graphitized diamond sample after the run end. Diamonds were placed between two successively compacted halves of NaCl powder poured into a split cylindrical mold, 8 mm in diameter and 7 mm high.

Prior to the experiment, the assembled high-pressure cell was dried at T = 120 °C for 10 h, then placed into the apparatus and sealed tightly; then water cooling for the interior power units was turned on. Pressure was created by oil pumping. The sample was heated by an electrical current through the graphite heater. After the required run duration, the samples were quenched by turning off the power. Quenching time was as short as 2–3 s due to efficient water cooling of the anvils. After the run, NaCl was dissolved in distilled water, and the extracted samples were dried. Details of the method were reported previously by Chepurov et al. (1998, 2012). The experiments were performed at a pressure of 2 GPa and a temperature of 1600 °C (run 4-6-16, duration 1 h) for surface graphite formation and at 1900 °C (run 4-12-16, duration 0.5 h) for bulk diamond-to-graphite phase change. In both cases, the particles expanded.

Samples A (graphite from an HMC sample), B (1600 °C, 2 GPa), and C (1900 °C, 2 GPa) were analyzed using a Bruker DUO single-crystal X-ray diffractometer (Debye-Scherrer camera, copper anode with microfocus X-ray tubes; 0.6-m collimator; 1024 × 1024 resolution of a charge-coupled device (CCD) detector; room temperature) following

the methods reported by Panchenko et al. (2014) and Yelisseyev et al. (2015). The detector was placed at 40 mm from the sample and tilted at an angle of $2\theta_d = -45°$ to the primary beam to investigate the scattering 2θ angles from 10 to 82°. LaB_6 (NIST SRM-660 ceramics) and Si–SRM-640A were used as external standards. The diffractometry strategy was designed in such a way as to set the sample successively in 94 different positions relative to the primary beam (χ and ω angles) to complete its rotation about the φ axis for the count time. Debye rings were stacked and displayed in the standard 2θ(I) form using XRD2DScan software (Rodriguez-Navarro, 2006). The correction for the external standard LaB_6 (NIST SRM-660a) was applied using Dioptas software (Prescher and Prakapenka, 2015).

This method allowed us to obtain standard X-ray diffraction patterns free from preferred crystal orientations and to perform a high-quality XRP analysis. The graphite contents in samples were estimated according to the relative intensities of graphite $(110)_G$ and diamond $(220)_D$ reflections. This pair of the reflections is rather well discriminated in the positions, and their reflection intensity ratio for the theoretical 1:1 mixture is quite acceptable. The PCW software (Kraus and Nolze, 1996) was applied for Rietveld refinement of the 70–82° 2θ interval.

Transmission spectra in the mid-IR were recorded using the Fourier-transform spectrometer Infralum 801. For local measurements we used a Vertex 70 FTIR spectrometer combined with a Hyperion 2000 microscope. The typical diameter of the beam was 50 to 100 μm. Raman spectra were recorded with a spectral resolution of 1 cm^{-1} at room temperature at excitations of 514.5 nm (Ar^+ laser) and 325 nm (He-Cd laser) using a confocal LabRam micro-Raman spectrometer. Raman spectroscopy is widely used to characterize diamond and different carbon materials; the details are described elsewhere (Tuinstra and Koenig, 1970; Wopenka and Pasteris, 1993; Jawhari et al., 1995; Frezzotti et al., 2012; Hatipoglu et al., 2012; http://www.dst.unisi.it/geofluids/raman/ spectrum_frame.htm). The surface morphology of the samples was investigated using optical microscopy (Olympus BX35) and scanning electron microscopy (SEM; 1540 XB Crossbeam, Carl Zeiss). To perform SEM analysis, a thin layer (10 Å) of aluminum was deposited on the surface of the samples by thermal evaporation in a vacuum. SEM images were obtained at an accelerating voltage of 20 kV using a secondary electron detector.

3. Results

Characterization of impact diamonds of the Popigai crater was performed. The impact diamonds are paramorphosis after graphite (Masaitis, 1998). As a result, they do not have their own crystallographic form, but inherit the shape of graphite grains. Figure 2 shows a particle of impact diamond with typical layering inherited from the original graphite.

The second main feature of the impact diamonds of the Popigai crater is that they represent an aggregate of nanoscale grains of the cubic diamond and hexagonal lonsdaleite phases (Figures 3 and 4). Raman spectroscopy of impact diamonds reveals variations in the spectra at different points, which indicates the nanometer structure domains. The most characteristic is the wide Raman peak with a maximum at 1300–1350 cm^{-1} and with a half-width of 19–23 cm^{-1}. The presence of amorphous carbon is recognized by the presence of a peak at 1600 cm^{-1}. Nanocrystalline graphite was identified. The spectra are consistent with our previously obtained data for impact diamonds (Yelisseyev et al., 2013).

X-ray diffraction study was performed on graphite particles from the Popigai crater and particles of impact diamond after high pressure annealing experiments. For Sample A, the X-ray diffraction pattern of the fixed sample (Laue geometry) shows the single-crystal structure of graphite particles (see inset in Figure 5a). No features concerning the interaction with a silicate tagamite melt were found.

For sample B (run 4-6-16, heating of impact diamond particles about 100 μm to 1600 °C at 2 GPa), the diffraction pattern (see inset in Figure 5b) shows graphite samples to be polycrystalline and there are also diamond reflections (possibly lonsdaleite). The diamond/graphite ratio is 90% / 10%. Note that the complex profile of the graphite $(002)_G$ reflection has been processed with OriginLab software (Lorentzian peak function) to show the peak positions at

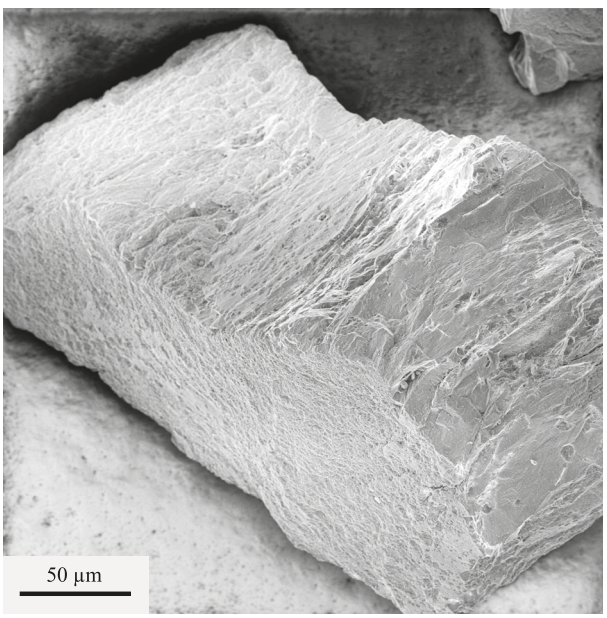

Figure 2. SEM image of impact diamond particle from the Popigai crater.

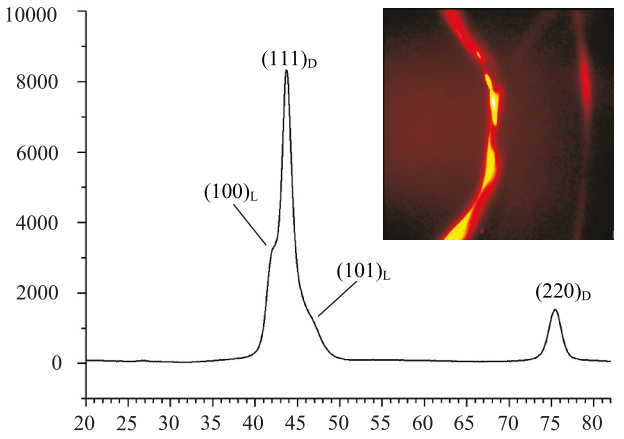

Figure 3. Diffraction pattern obtained with a Bruker DUO diffractometer (Debye-Scherrer geometry, CuKα-radiation, microfocus X-ray source): diamond particles from the Popigai crater.

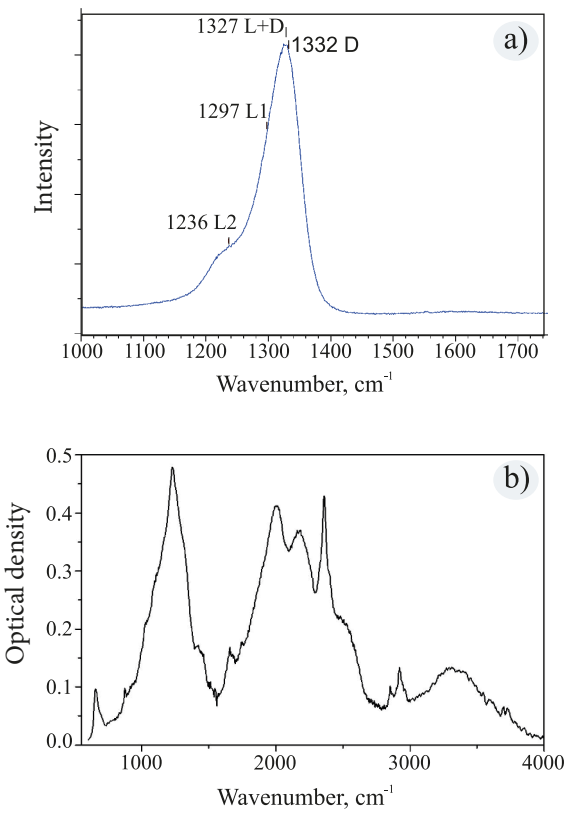

Figure 4. Raman spectrum (a) and IR spectrum (b) of impact diamond particle from the Popigai crater.

26.58 (d = 3.35 Å) for the main line and 27.76° 2θ (d = 3.21 Å) for the satellite line. The tabulated values for the graphite (002) reflection are 2θ = 26.58°, d = 3.35 Å (ICDD, 2009), and the half-widths (FWHM) of the lines are 0.9° and 1.2° 2θ, respectively. The broadening of the lines relative to the LaB_6 standard (ceramics NIST SRM-660, FWHM = 05° 2θ) allows us to estimate the sizes of coherently scattering domains as 23 and 13 nm, respectively.

The low value of d_{002} = 3.21 may be associated with the formation of the compressed graphite (pressurized graphite in the diamond matrix). Such satellite lines were recorded at the $(002)_G$ reflections in synthetic lonsdaleite (Bundy and Casper, 1966), with the unit cell parameters in the range of 3.10–3.15 Å. X-ray analysis of sample C synthesized at 2 GPa and 1900 °C shows that all impact diamond particles have been transformed into graphite; no diamond reflections were detected (see inset in Figure 5c). The FWHM of the graphite reflections are much greater (about three times), but this cannot be correlated reliably with the increased coherent scattering domain because of the significant difference in the size of A and C particles.

4. Discussion

Graphite can form either on the surface of a single-crystal diamond or by phase change of bulk diamond. Surface graphite formation is essentially a catalytic chemical reaction basically different from and not connected with a purely physical phase change (polymorphic diamond-to-graphite conversion). Both chemical and physical processes, respectively, occur within the P-T field of diamond stability, but the phase change requires a higher temperature than graphite formation on the surface. In vacuum and at low oxygen partial pressure, the temperature boundary between the two processes is from 1600 to 1700 °C (Seal, 1958; Evans and James, 1964). Surface graphite formation is often called low-temperature graphitization.

According to Evans and Sauter (1961), graphite forms on diamond surfaces by deposition of nondiamond carbon resulting from diamond etching by catalytic gas agents (O_2, H_2O, CO_2), though any environmental component capable of chemically reacting with diamond can act as a catalyst. The process is possible due to dynamic equilibrium between etching (oxidation) of diamond and deposition of nondiamond carbon on its surface, which converts to graphite at high temperatures (Sonin et al., 2000). Nucleation and growth of graphite on the diamond surface at low temperature was described by Khmelnitsky and Gippius (2013).

Diamond oxidation within the thermodynamic stability of graphite generally comprises multiple stages (Phaal, 1965): 1) direct oxidation to CO and CO_2 (reaction rate R_1); 2) formation of a film of amorphous carbon on the diamond surface (R_2); and 3) direct oxidation of the carbon film (R_3). Stage 2 is actually the stage of surface

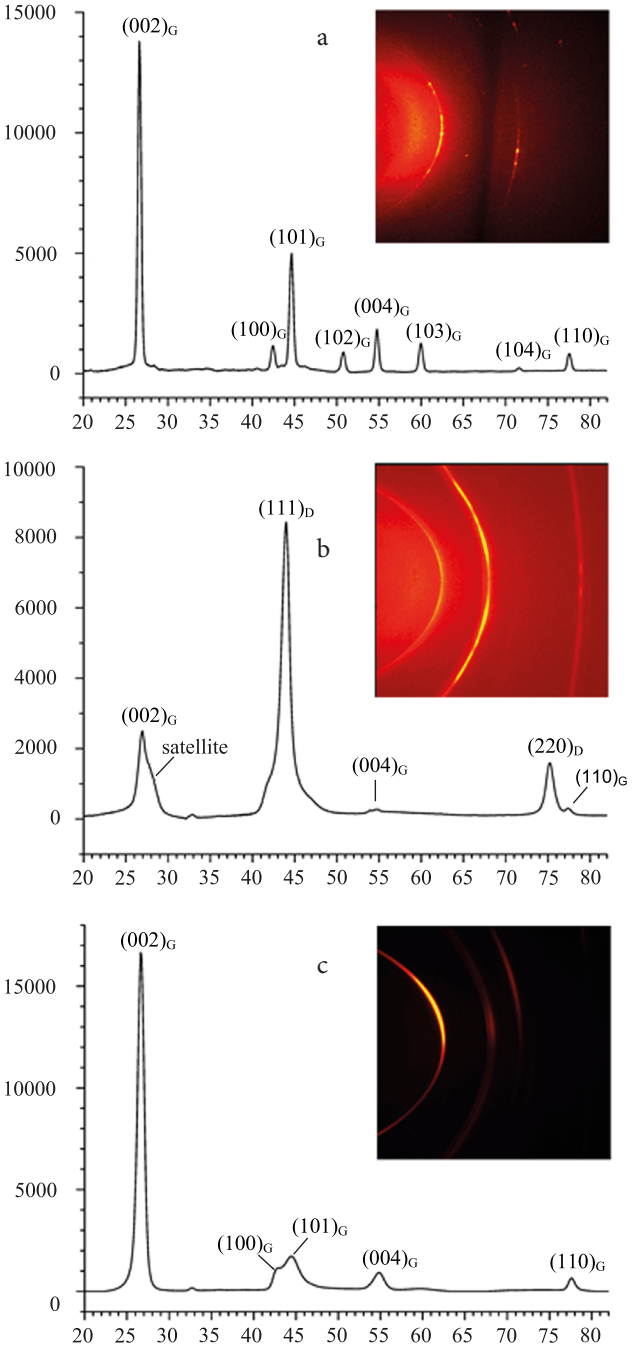

Figure 5. Diffraction patterns obtained with a Bruker DUO diffractometer (Debye-Scherrer geometry, CuKα-radiation, microfocus X-ray source). a) Graphite particles from the Popigai crater; b) particle obtained at heating to 1600 °C and 2 GPa; c) fully graphitized particle of impact diamond (1900 °C, 2 GPa). Numerals in brackets correspond to graphite reflection peaks. Insets show diffraction patterns of fixed samples.

graphite formation. For instance, at $R_2 >> R_3$, a thick coat of nondiamond carbon forms around diamond crystals. Graphite formation initiates on crystal edges but develops preferably on growth steps, etch pits, and cracks on the faces.

Nucleation of graphite inside a diamond by phase change is a spontaneous high-temperature process that starts at impurities and structure defects. The physical process is much faster than the chemical one (Andreev, 1999), and the rates of both are directly proportional to temperature and, possibly, inversely proportional to total pressure (Qian et al., 2004 ; Sonin et al., 2013).

An impact diamond, an aggregate of nanometer grains of high-pressure carbon (cubic diamond or hexagonal lonsdaleite), dramatically differs from the ordinary single-crystal diamond. Impact diamonds consist of tightly bound nanocrystals (5–50 nm) of cubic diamond and a small amount of lonsdaleite and preferred crystallographic orientations along the stacking direction (c-axis) of the source graphite. The structure of the Popigai diamonds was studied by Ohfuji et al. (2015, 2017). Therefore, graphite formation both on the diamond surface and as bulk diamond conversion can be expected to produce polycrystalline graphite. By comparing its structure with that of graphite from tagamite, one can see whether the latter results from graphitization or is a residual phase that survived conversion to diamond during the impact event. Impact diamond may undergo phase change at a lower temperature due to its highly disordered polycrystalline structure with particle sizes of tens to a few hundreds of nanometers.

As we expected, graphitization of impact diamonds yielded microcrystalline graphite aggregates, whereas graphite from the tagamite concentrate is well ordered and monocrystalline. Therefore, tagamite contains residual graphite not converted to diamond during the meteorite impact.

In this respect, the question arises of why diamond paramorphosis after graphite and residual graphite (not converted to high-pressure phases) coexist in a small amount of concentrated tagamite, within a limited space where conditions between the impact event and cooling of the tagamite melt were identical. This was explained by experiments performed at the Institute for Superhard Materials in Kyiv (Britun et al., 2003). Namely, lonsdaleite together with cubic diamond and residual graphite were obtained in experiments with highly ordered pyrolytic graphite using Bridgman toroidal anvil pressure cells at 7.7 GPa and 1500 °C. Residual graphite remained after 30% of graphite converted to dense phases by a nondiffusion mechanism during the impact (Britun et al., 2003). The conversion occurs as deformation-induced lattice change of the original material. Graphite crystals in strongly deformed gneisses of the Khapchan Group had different

orientations relative to the impact stress direction. Graphite deforms most strongly if its base plane is nearly normal to the impact direction, which is optimal for the formation of dense phases (lonsdaleite and cubic diamond, the latter being the predominant phase). If the base plane is oblique to the impact direction, stress releases by the sliding of graphite layers along this plane, and no dense phases can form. As a result, impact events can produce either impact diamonds almost free from lonsdaleite or combinations of lonsdaleite-cubic diamond-residual graphite, with remnant original graphite, depending on the crystal orientations of the source graphite.

Visually and in terms of aggregation, samples of impact diamonds are close to carbonado samples, but there are significant differences (Haggerty, 2017). Impact diamonds of the Popigai crater are an aggregate of cubic and hexagonal (lonsdaleite) diamonds, and carbonado is an exclusively cubic diamond. Impact diamonds do not have their own crystallographic shape, since they are paramorphosis after graphite. Microcrystals from carbonado aggregates are crystals of octahedral and cuboctahedral habit, being a typical diamond with cubic structure. Figure 6a shows a carbonado sample from Brazil, and Figure 6b shows an aggregate of diamond crystals after dissolving the silicate components from the carbonado sample. It is clearly seen that diamond crystals are cuboctahedrons with secondary faces of a rhombododecahedron. At the same time, the faces of the octahedron and rhombododecahedron are flat, and the cubic faces are rough, consisting of pits and hillocks. Such morphology of diamond is often observed among diamonds from mantle xenoliths of eclogites from kimberlites (Afanasiev et al., 2000).

5. Conclusions

As the reported study shows, both surface graphite formation on impact diamond and its bulk phase change produce polycrystalline graphite with particles commensurate to those in the source diamond, while the graphite from concentrated tagamite that encloses impact diamond is monocrystalline. Therefore, graphite in tagamite is a residual phase that has survived conversion to high-pressure phases during the impact event rather than being of retrograde origin (back-conversion of impact diamond to graphite in a high-temperature tagamite melt). Etching (catalytic oxidation) is the basic way of studying diamond interaction with tagamite melt (Walter et al., 1992). Coexistence of lonsdaleite, cubic diamond, and single-crystal graphite within a limited volume may be due to different orientations of the graphite base plane relative to the impact stress direction. High-pressure phases form at the base plane normal to the impact and cannot form at smaller oblique angles as stress releases by sliding along the graphite base plane. Thus, the diamond-bearing rocks may contain significant amounts of residual graphite.

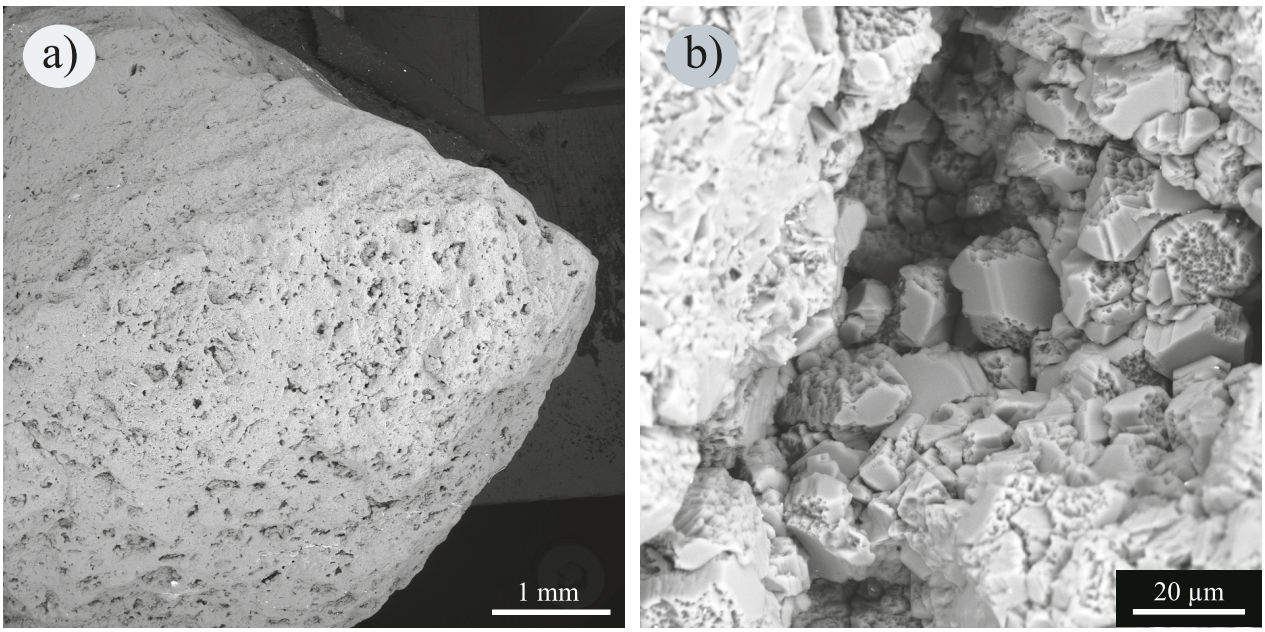

Figure 6. Carbonado (Brazil): a) general view; b) diamond microcrystals in carbonado pores after removal of mineral phases by dissolution.

Acknowledgments

The authors thank the Editorial Board of the Turkish Journal of Earth Sciences for handling of the manuscript. The authors thank an anonymous referee and Prof Dr Murat Hatipoğlu for comprehensive reviewing that resulted in significant improvement of the manuscript. The work was partially supported by Grant 16-05-00873 from the Russian Foundation for Basic Research and was carried out as a part of Project No. 0330-2016-0006. Valeri Sonin and Egor Zhimulev thank the Russian Science Foundation for support of experimental works (Grant No. 17-17-01154). Aleksei Chepurov thanks the state assignment project no. 0330-2016-0012 for support of analytical works.

References

Afanasiev VP, Yefimova ES, Zinchuk NN, Koptil VI (2000). Atlas of Morphology of Diamonds from Russian Sources. Novosibirsk, Russia: SPC UIGGM SB RAS.

Andreev VD (1999). Spontaneous graphitization and thermal disintegration of diamond at >2000K. Physics of the Solid State 41: 627-632.

Britun VF, Kurdyuiumov AV, Petrusha IA (2003). Nucleation of dense phases upon compaction of hexagonal graphite: structural features. Sverkhtverdye Materialy 5: 11-18.

Bundy FP, Casper JS (1966). Hexagonal diamond – a new form of carbon. Journal of Chemical Physics 44: 181-184.

Chepurov AI, Fedorov II, Sonin VM (1998). Experimental studies of diamond formation at high PT-parameters (supplement to the model for natural diamond formation). Geologiya i Geofizika 39: 234-244.

Chepurov AI, Tomilenko AA, Zhimulev EI, Sonin VM, Chepurov AA et al. (2012). The conservation of an aqueous fluid in inclusions in minerals and their interstices at high pressures and temperatures during the decomposition of antigorite. Russian Geology and Geophysics 53: 234-246.

Evans T, James PF (1964). A study of the transformation of diamond to graphite. Proceedings of the Royal Society A277: 260-269.

Evans T, Sauter DH (1961). Etching of diamond surfaces with gases. Philosophical Magazine 6: 429-440.

Frezzotti ML, Tecce F, Casagli A (2012). Raman spectroscopy for fluid inclusion analysis. Journal of Geochemical Exploration 112: 1-20.

Galimov E (1984). Variations in the isotope composition of diamonds and their relation to the conditions of diamond formation. Geokhimiya 8: 34-41 (in Russian).

Haggerty SE (2017). Carbonado diamond: a review of properties and origin. Gems and Gemology 53: 168-179.

Hatipoglu M, Ajo D, Kibici Y, Passeri D (2012). Natural carbon black (Oltu-stone) from Turkey: a micro-Raman study. Neues Jahrbuch für Mineralogie - Abhandlungen 189: 97-101.

Hemingway BS, Bohlen SR, Hankins WB, Westrum EF Jr, Kuskov OL (1998). Heat capacity and thermodynamic properties for coesite and jadeite, reexamination of quartz-coesite equilibrium boundary. American Mineralogist 83: 409-418.

ICDD (2009). Powder Diffraction File. PDF-2/Release 2009. Newtown Square, PA, USA: International Centre for Diffraction Data, 2009.

Jawhari T, Roig A, Casado J (1995). Raman spectroscopic characterization of some commercially available carbon black materials. Carbon 33: 1561-1565.

Kennedy CS, Kennedy GC (1976). The equilibrium boundary between graphite and diamond. Journal of Geophysical Research 81: 2467-2470.

Khmelnitsky RA, Gippius AA (2013). Transformation of diamond to graphite under low pressure. Phase Transit 87: 175-192.

Kraus W, Nolze G (1996). POWDER CELL – A program for the representation and manipulation of crystal structures and calculation of the resulting X-ray powder patterns. Journal of Applied Crystallography 29: 301-303.

Kryukov VA, Tolstov AV, Afanasiev VP, Samsonov NYu, Kryukov YaV (2016). Ensuring the Russian high-tech industry resources by products based on giant fields of the arctic – Tomtor niobium-rare-Earth and ultra-hard abrasive Popigai material. Interexpo GEO-Siberia 3: 188-192 (in Russian).

Masaitis VL (editor) (1998). Diamond-bearing Impactites of the Popigai Astrableme. St. Petersburg, Russia: VSEGEI (in Russian).

Masaitis VL (2014). Impact diamonds of the Popigai astrobleme: main properties and practical use. Geology of Ore Deposits 55: 607-612.

Nalivkin DV (editor) (2007). Geological Map of the Russian Federation. St. Petersburg, Russia: VSEGEI.

Ohfuji H, Irifune T, Litasov KD, Yamashita T, Isobe F et al. (2015). Natural occurrence of pure nano-polycrystalline diamond from impact crater. Scientific Reports 5: 14702.

Ohfuji H, Nakaya M, Yelisseyev AP, Afanasiev VP, Litasov KD (2017). Mineralogical and crystallographic of polycrystalline yakutite diamond. Journal of Mineralogical and Petrological Sciences 112: 46-51.

Panchenko AV, Tolstykh ND, Gromilov SA (2014). The technique of X-ray diffraction investigation of crystal aggregates. Zhurnal Strukturnoi Khimii 55 (Suppl. 1): S73-S78.

Phaal C (1965). Surface studies of diamond I. Industrial Diamond Review 25: 486-489.

Prescher C, Prakapenka VB (2015). DIOPTAS: A program for reduction of two-dimensional X-ray diffraction data and data exploration. High Pressure Research 35: 223-230.

Qian J, Pantea C, Huang J, Zerda TW, Zhao Y (2004). Graphitization of diamond powders of different sizes at high pressure-high temperature. Carbon 42: 2691-2697.

Rodriguez-Navarro A (2006). XRD2D Scan: new software for polycrystalline materials characterization using two-dimensional X-ray diffraction. Journal of Applied Crystallography 39: 905-909.

Seal M (1958). Graphitization and plastic deformation of diamond. Nature 182: 1264-1267.

Shul'zhenko AA, Ashkinazi EE, Sokolov AN, Petasyuk GA, Aleksandrova LI et al. (2014). Structure and properties of impact diamonds from the Popigai Deposit and polycrystals based on them. Journal of Superhard Materials 36: 156-164 (in Russian).

Sonin VM, Chepurov AI, Zhimulev EI, Chepurov AA, Sobolev NV (2013). Surface graphitization of diamond in K_2CO_3 melt at high pressure. Doklady Earth Sciences 451: 858-860.

Sonin VM, Fedorov II, Pokhilenko LN, Pokhilenko NP (2000). Diamond oxidation rate as related to oxygen fugacity. Geology of Ore Deposits 42: 496-502.

Tuinstra F, Koenig JL (1970). Raman spectrum of graphite. Journal of Chemical Physics 53: 1126-1132.

Walter AA, Eryomenko GK, Kvasnitsa VN, Polkanov YuA (1992). Carbon Minerals Produced by Impact Metamorphism. Kyiv, Ukraine: Naukova Dumka (in Russian).

Wopenka B, Pasteris JD (1993). Structural characterization of kerogens to granulite-facies graphite – applicability of Raman microprobe spectroscopy. American Mineralogist 78: 533-557.

Yelisseyev AP, Afanasiev VP, Panchenko AV, Gromilov SA, Kaichev VV et al. (2016). Yakutites: Are they impact diamonds from the Popigai crater? Lithos 265: 278-291.

Yelisseyev A, Khrenov A, Afanasiev V, Pustovarov V, Gromilov S et al. (2015). Luminescence of natural carbon nanomaterials — impact diamonds from the Popigai astrobleme. Diamond and Related Materials 58: 69-77.

Yelisseyev A, Meng GS, Afanasiev V, Pokhilenko N, Pustovarov V et al. (2013). Optical properties of impact diamonds from the Popigai astrobleme. Diamond and Related Material 37: 8-16.